Supporting Information

Promoting antitumor efficacy by suppressing hypoxia via nano self-assembly of two irinotecan-based dual drug conjugates owning a HIF-1α inhibitor

Bin Zhang,‡[ab] Xiaochao Huang,‡[ab] Hengshan Wang*[c] and Shaohua Gou*[ab]

[a.] *Pharmaceutical Research Center and School of Chemistry and Chemical Engineering, Southeast University, Nanjing 211189, China*

[b.] *Jiangsu Province Hi-Tech Key Laboratory for Biomedical Research, Southeast University, Nanjing 211189, China. E-mail: sgou@seu.edu.cn*

[c.] *State Key Laboratory for the Chemistry and Molecular Engineering of Medicinal Resources, School of Chemistry and Pharmaceutical Sciences, Guangxi Normal University, Guilin 541004, China. E-mail: whengshan@163.com*

‡ These authors contributed equally to this work.

Table S1 Cytotoxic effects of Ir, YC-1, Ir/YC-1 mixture, Ir-YC-1 and Ir-PEG_3-YC-1 NPs against LO2 cells (human normal liver cells) under normoxic and hypoxic conditions.

Compd.	IC_{50} (μM)	IC_{50} (μM)
	LO2 (Normoxic)	LO2 (Hypoxic)
Ir-YC-1 NPs	21.54 ± 0.45	28.15 ± 0.46
Ir-PEG_3-YC-1 NPs	24.63 ± 0.57	30.10 ± 0.83
Ir	18.90 ± 0.92	26.32 ± 1.31
YC-1	>80	>80
Ir/YC-1 mixture	18.42 ± 0.52	25.58 ± 0.80

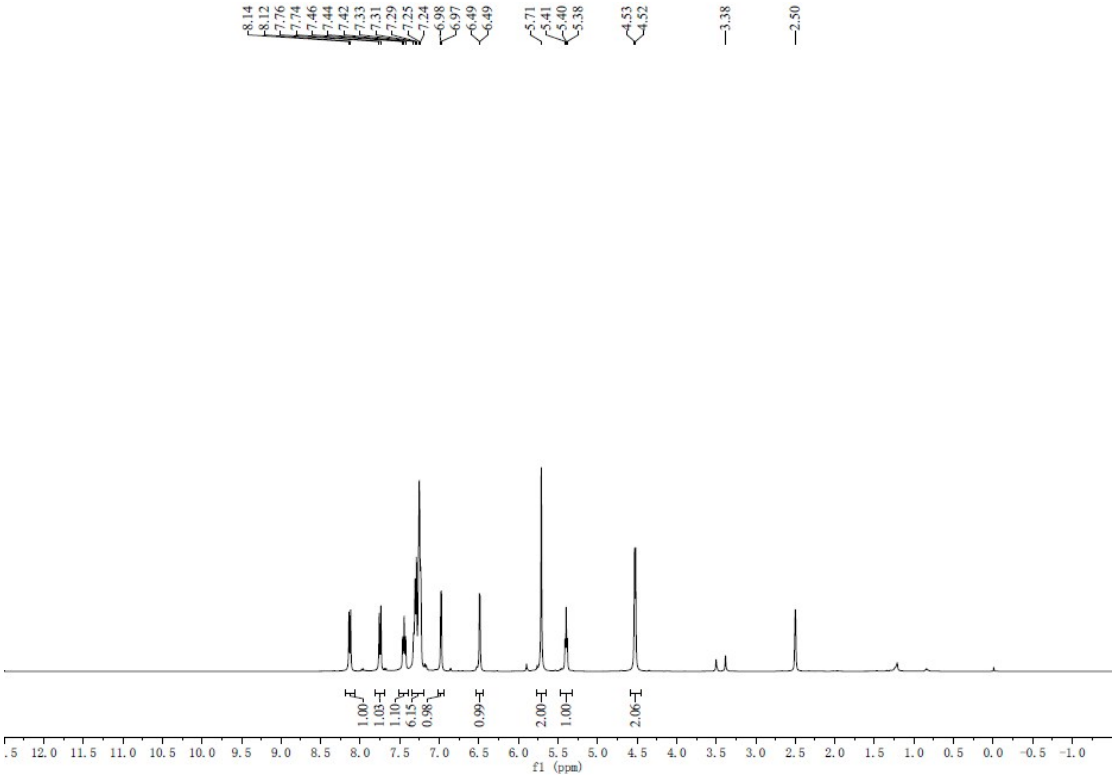

Figure S1. ^1H NMR spectrum of YC-1(400 MHz, DMSO-d_6).

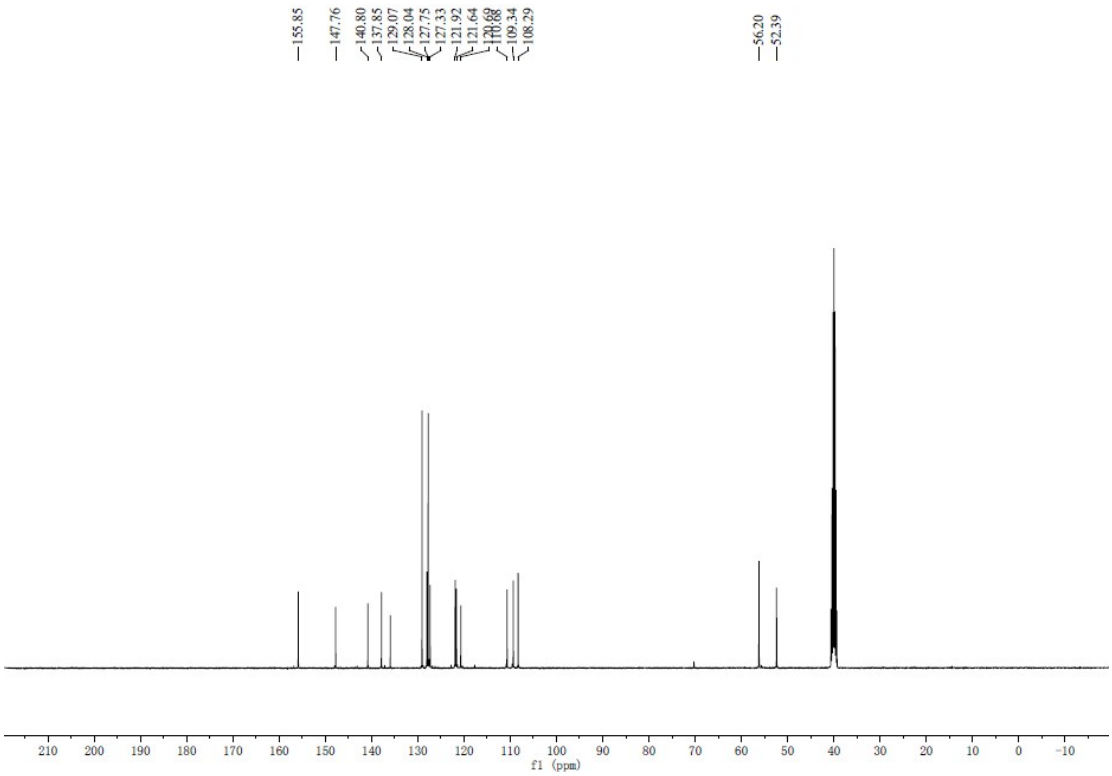

Figure S2. ^{13}C NMR spectrum of YC-1 (100 MHz, DMSO-d_6).

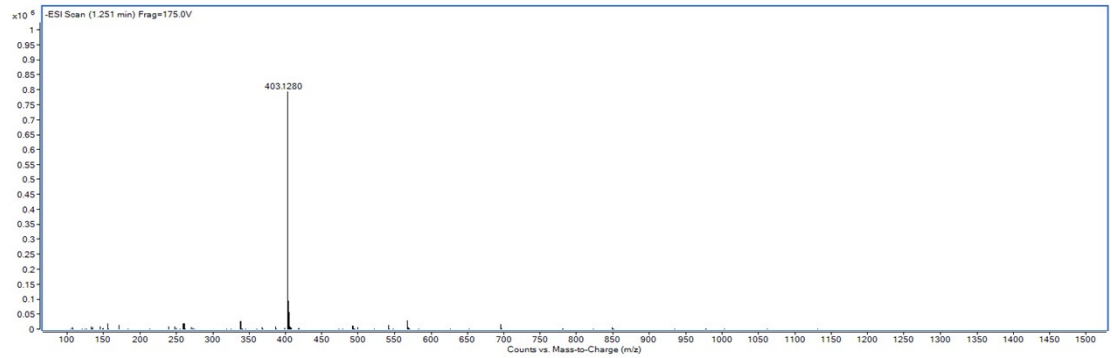

Figure S3. ESI-MS mass spectrum of YC-1.

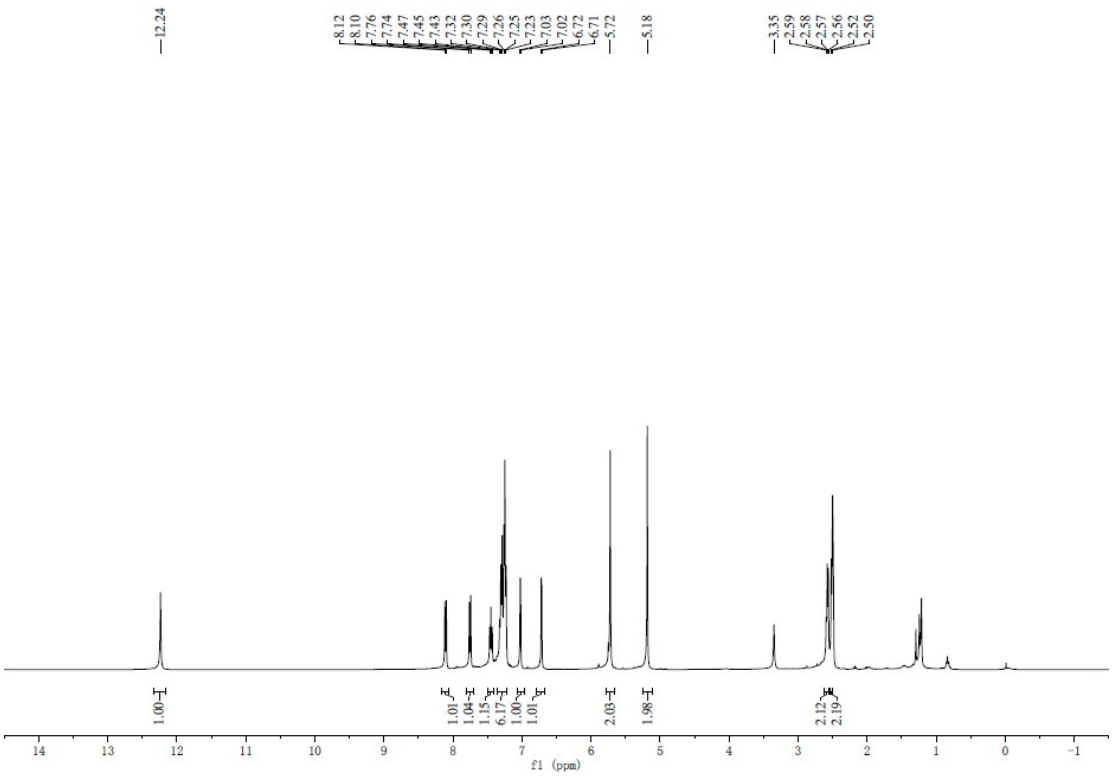

Figure S4. ^{1}H NMR spectrum of YC-2 (400 MHz, DMSO-d_6).

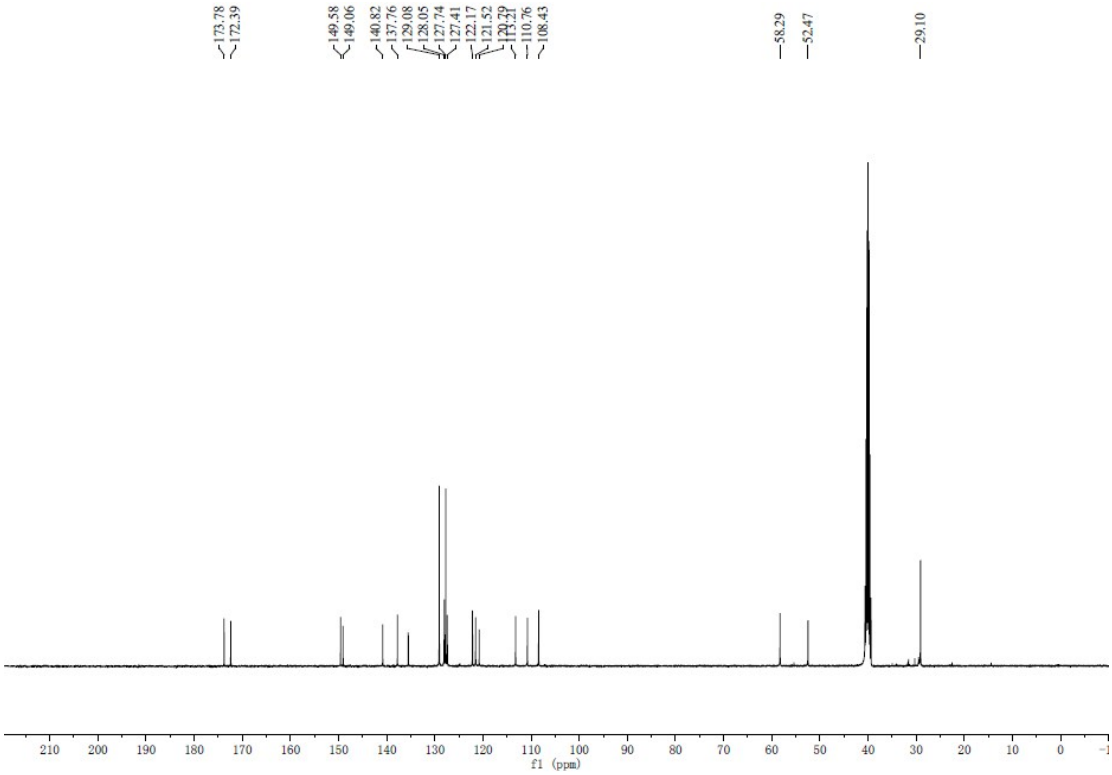

Figure S5. ^{13}C NMR spectrum of YC-2 (100 MHz, DMSO-d_6).

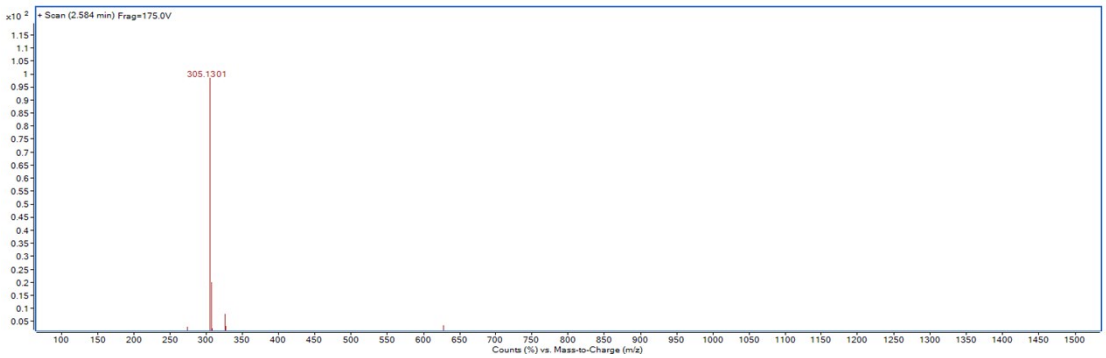

Figure S6. ESI-MS mass spectrum of YC-2.

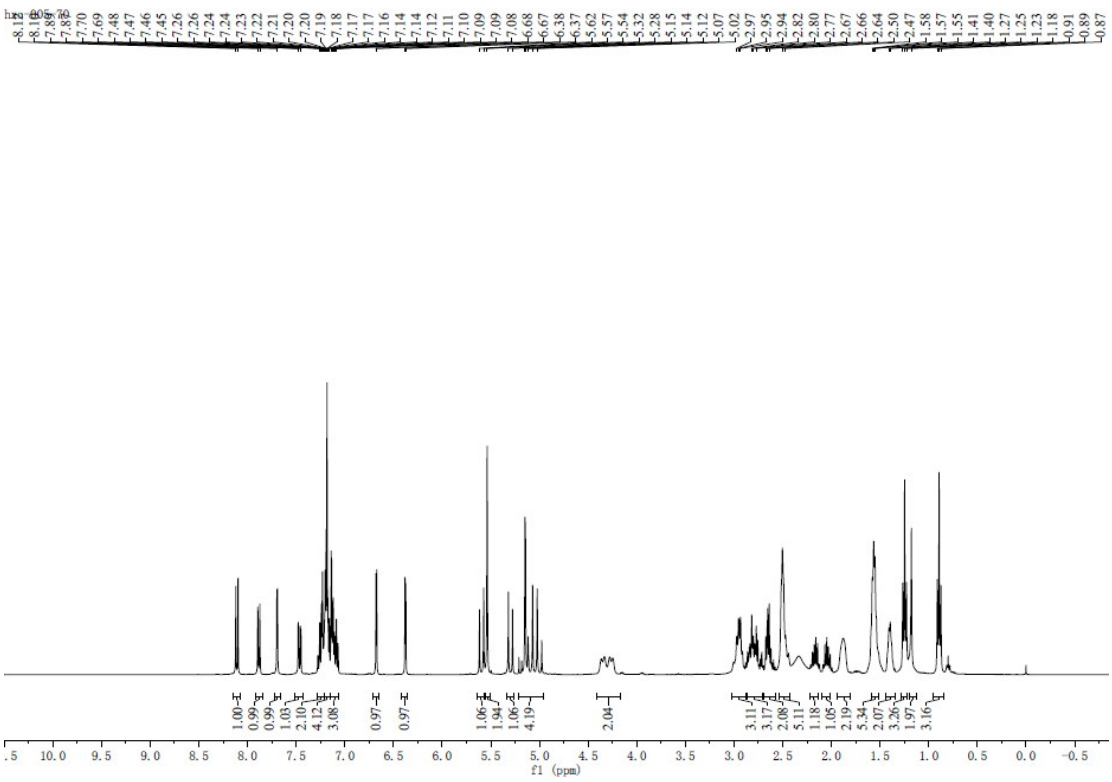

Figure S7. ^{1}H NMR spectrum of Ir-YC-1 (400 MHz, $CDCl_3$).

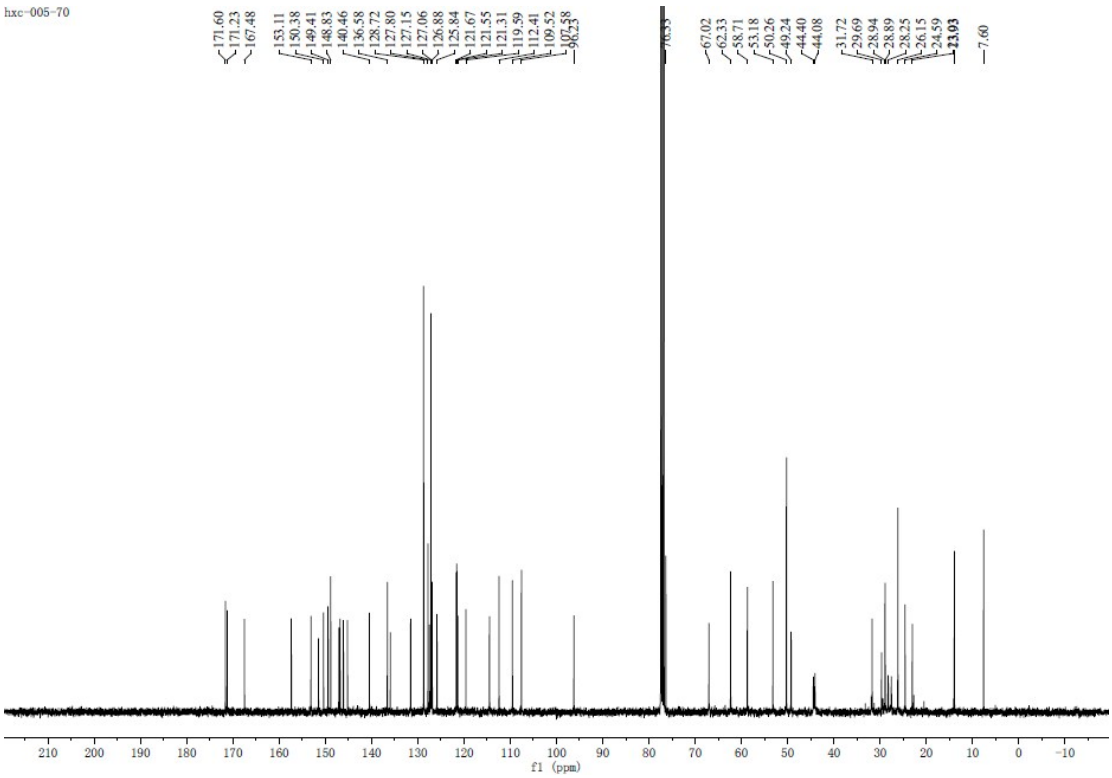

Figure S8. ^{13}C NMR spectrum of Ir-YC-1(100 MHz, $CDCl_3$).

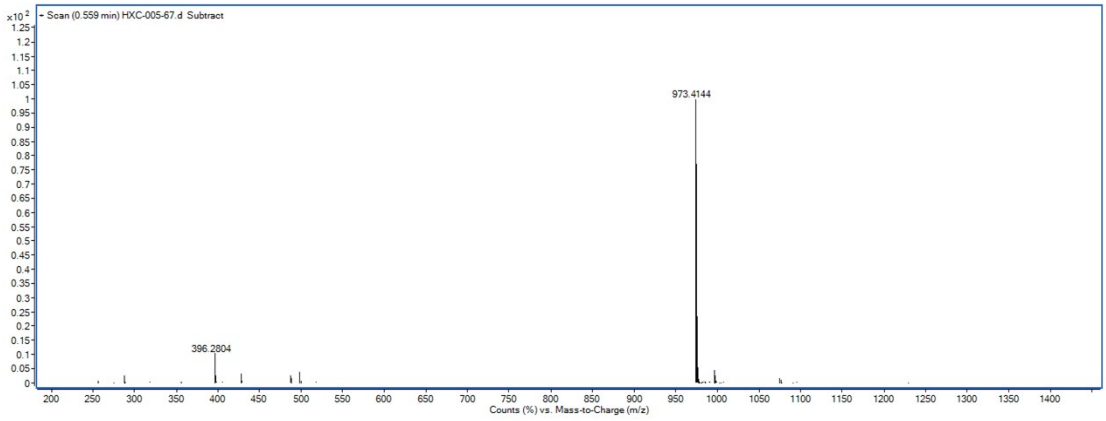

Figure S9. ESI-MS mass spectrum of Ir-YC-1.

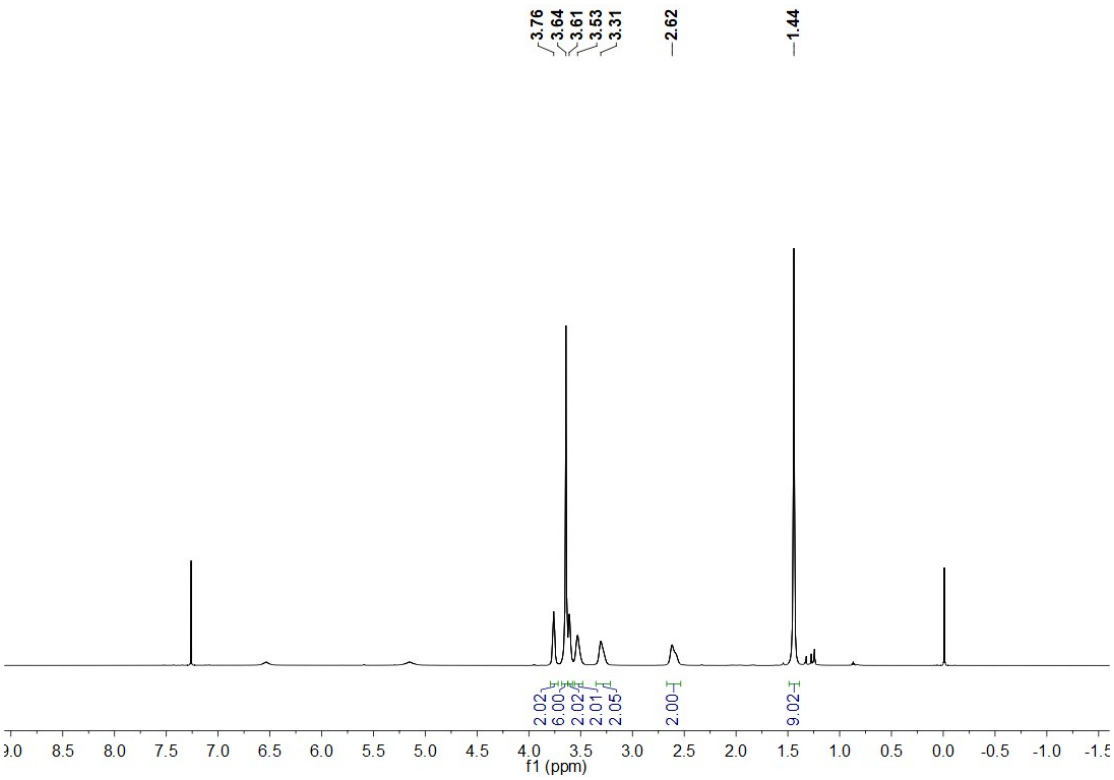

Figure S10. ^{1}H NMR spectrum of compound 2 (400 MHz, $CDCl_3$).

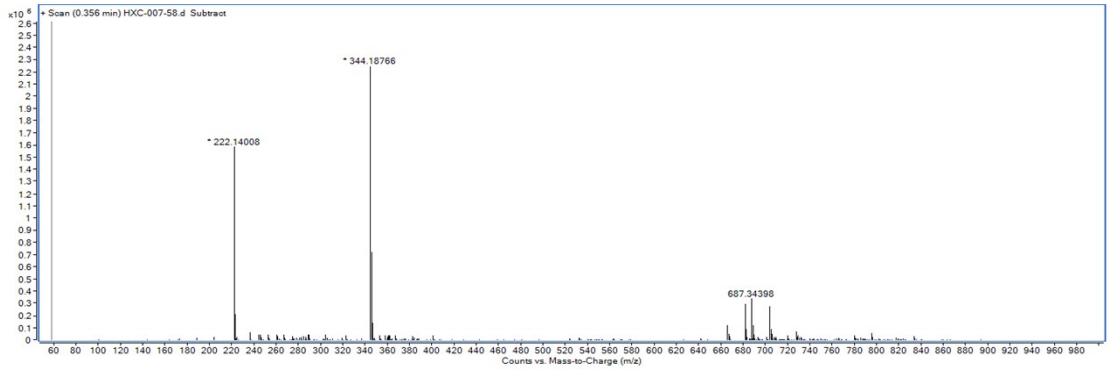

Figure S11. ESI-MS mass spectrum of compound 2.

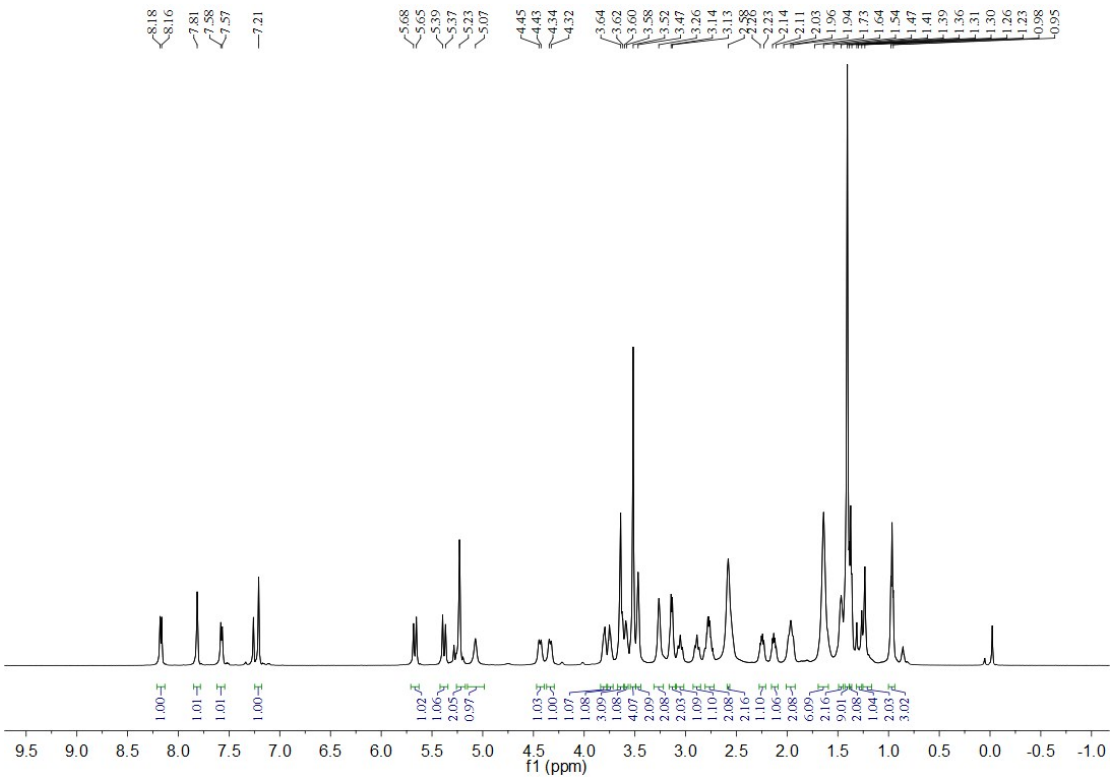

Figure S12. ^{1}H NMR spectrum of compound 3 (400 MHz, $CDCl_3$).

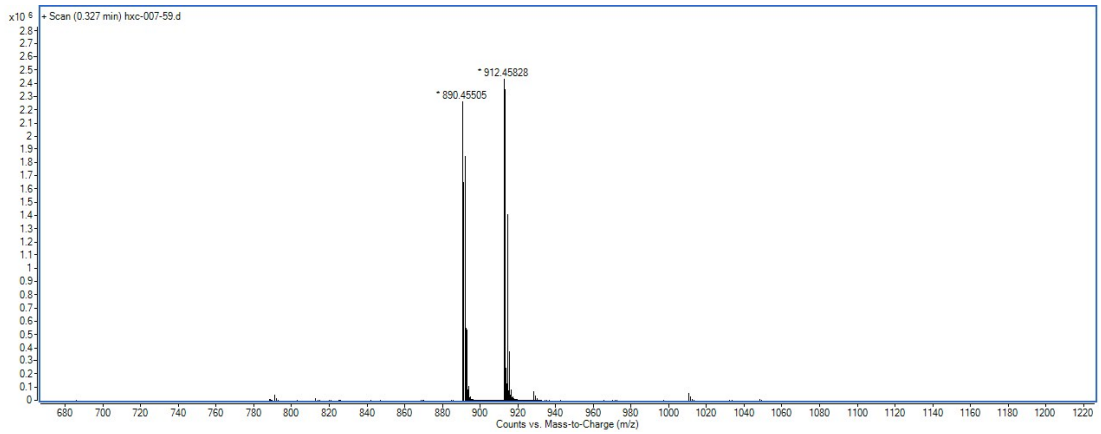

Figure S13. ESI-MS mass spectrum of compound 3.

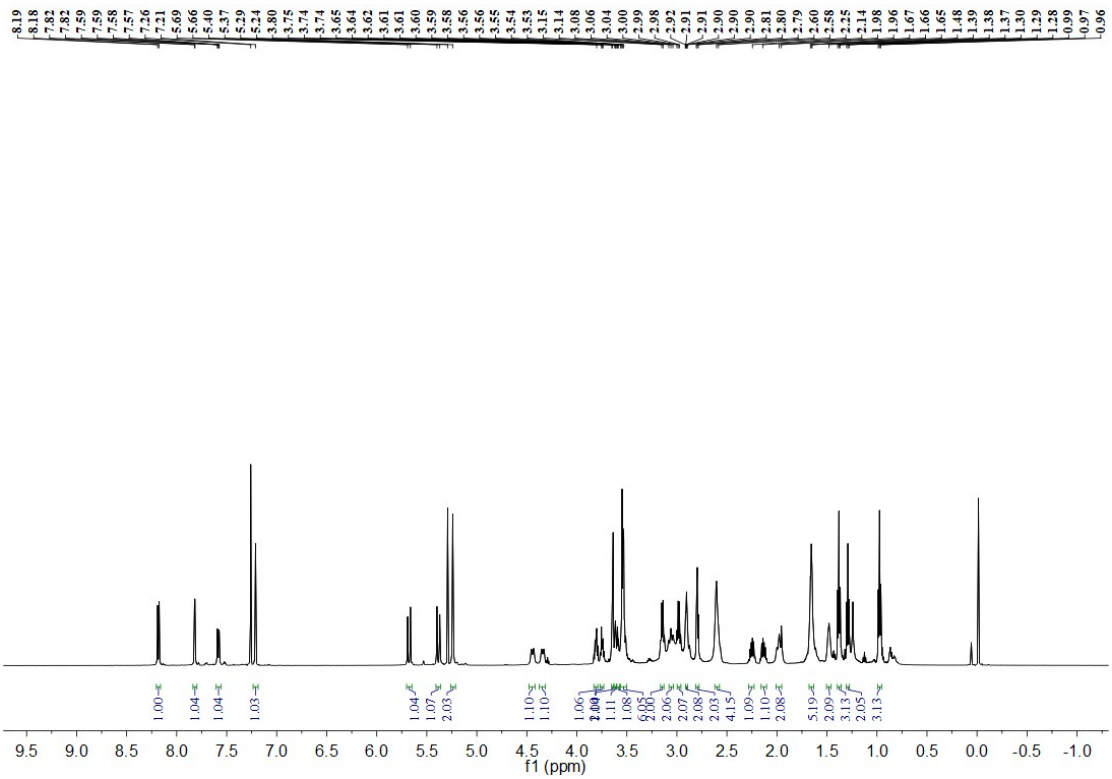

Figure S14. ^{1}H NMR spectrum of compound 4 (400 MHz, $CDCl_3$).

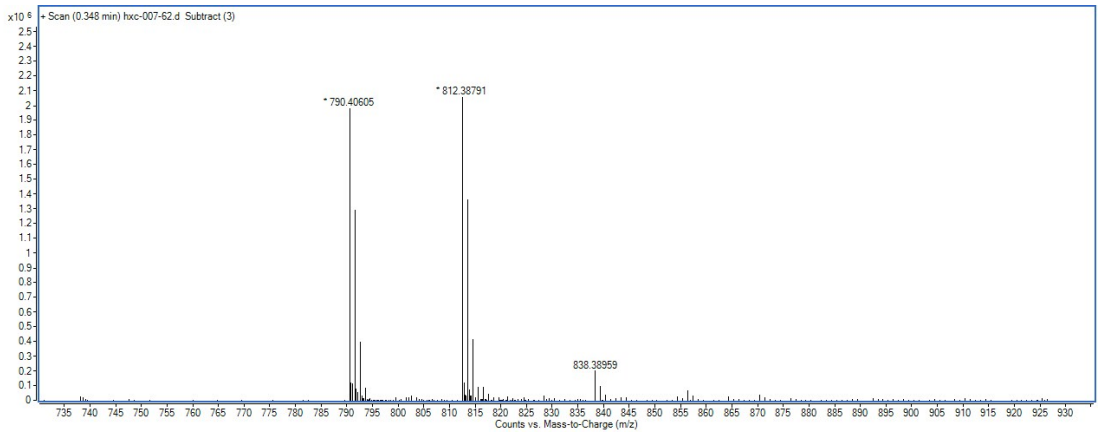

Figure S15. ESI-MS mass spectrum of compound 4.

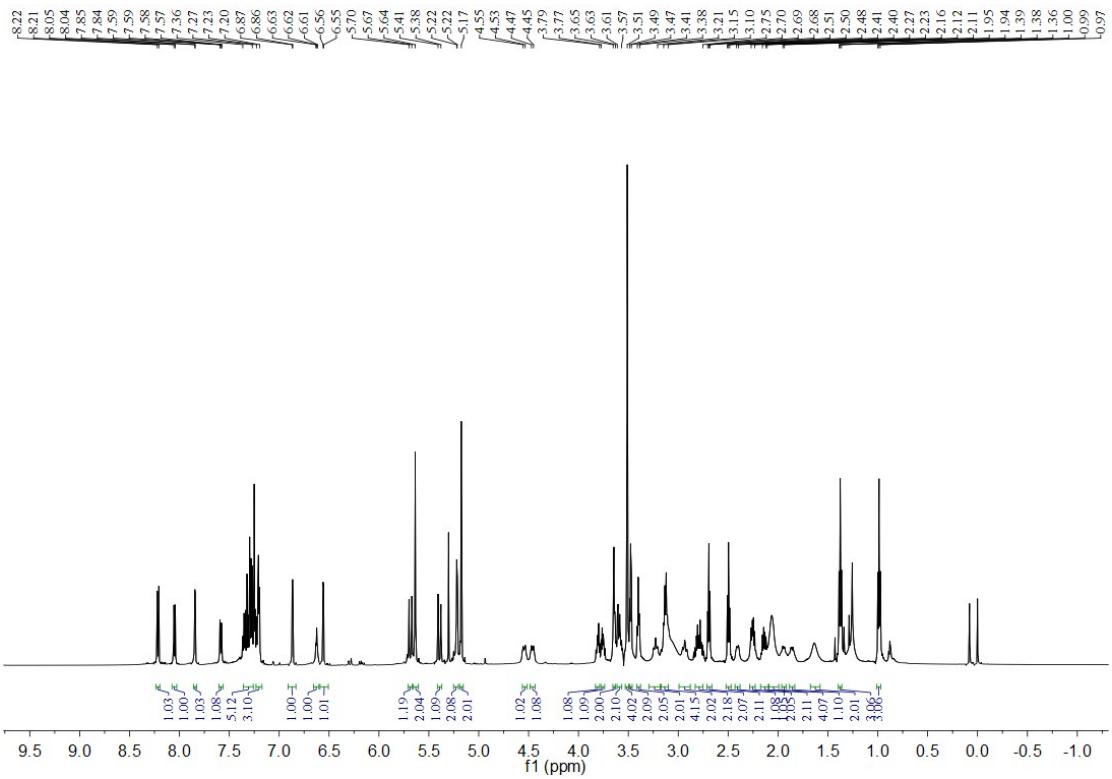

Figure S16. ^{1}H NMR spectrum of Ir-PEG_3-YC-1 NPs (400 MHz, $CDCl_3$).

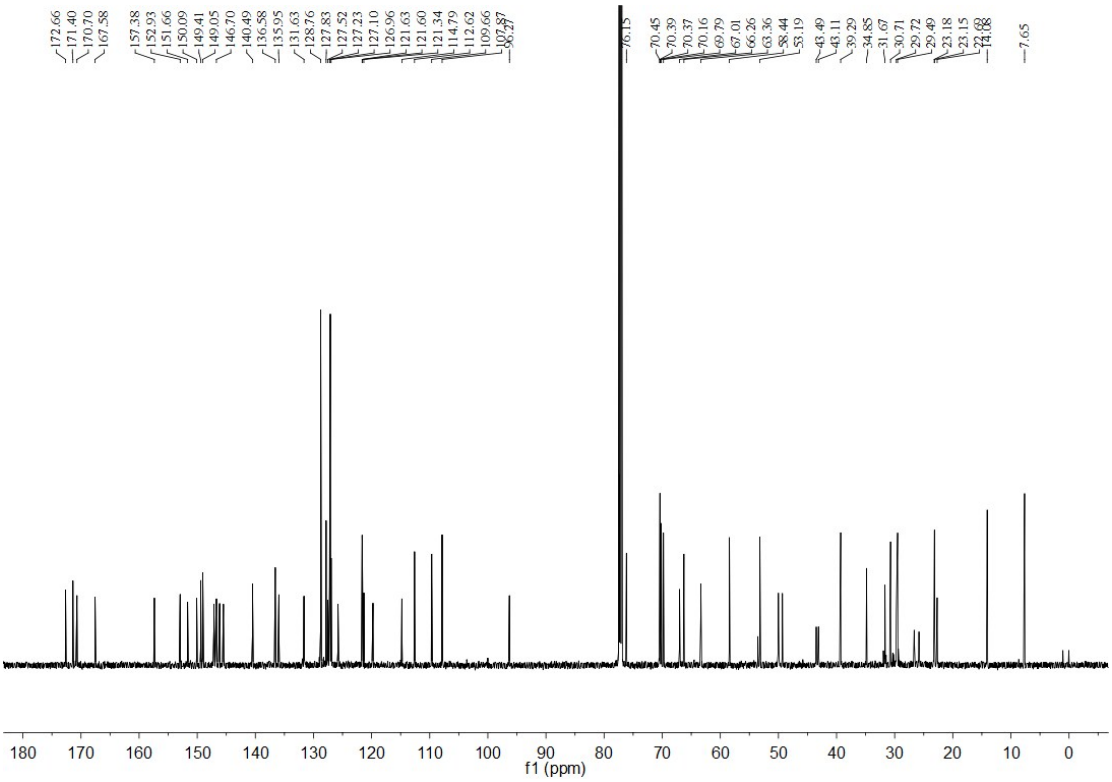

Figure S17. ^{13}C NMR spectrum of Ir-PEG_3-YC-1(100 MHz, $CDCl_3$).

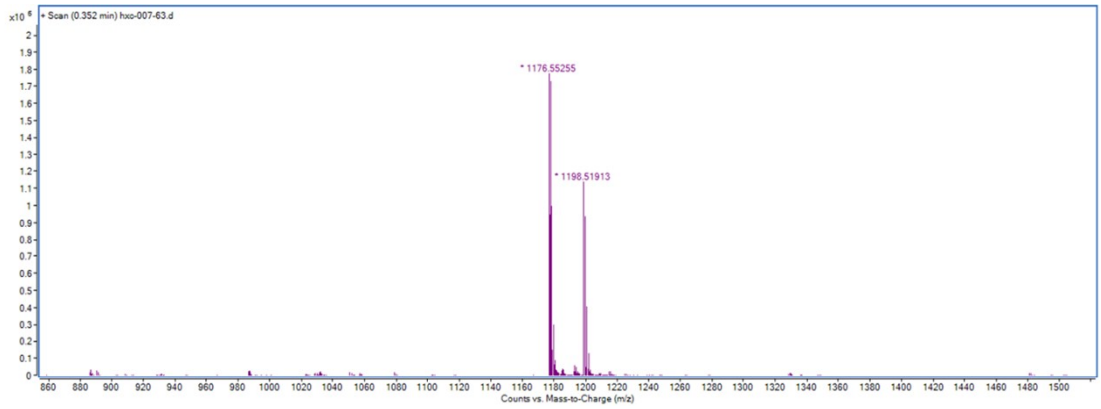

Figure S18. ESI-MS mass spectrum of Ir-PEG_3-YC-1 NPs.

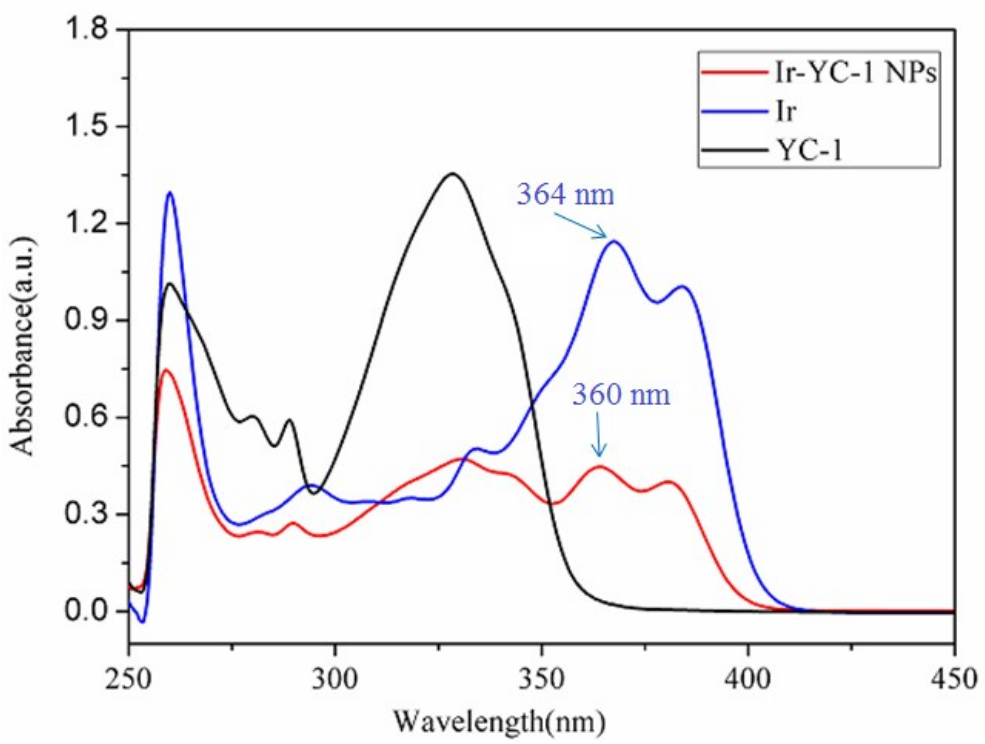

Figure S19. UV/Vis spectra of Ir, YC-1 and Ir-YC-1 NPs in acetonitrile.

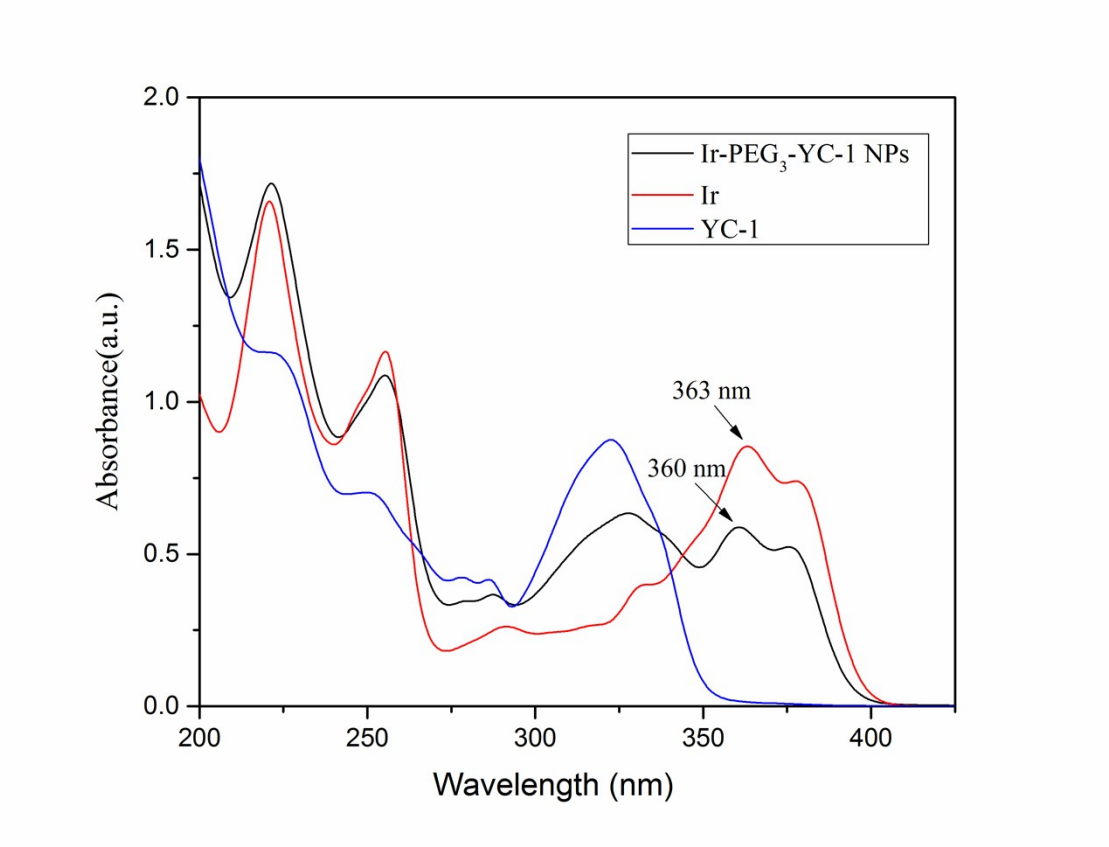

Figure S20. UV/Vis spectra of Ir, YC-1 and Ir-PEG_3-YC-1 NPs in acetonitrile.

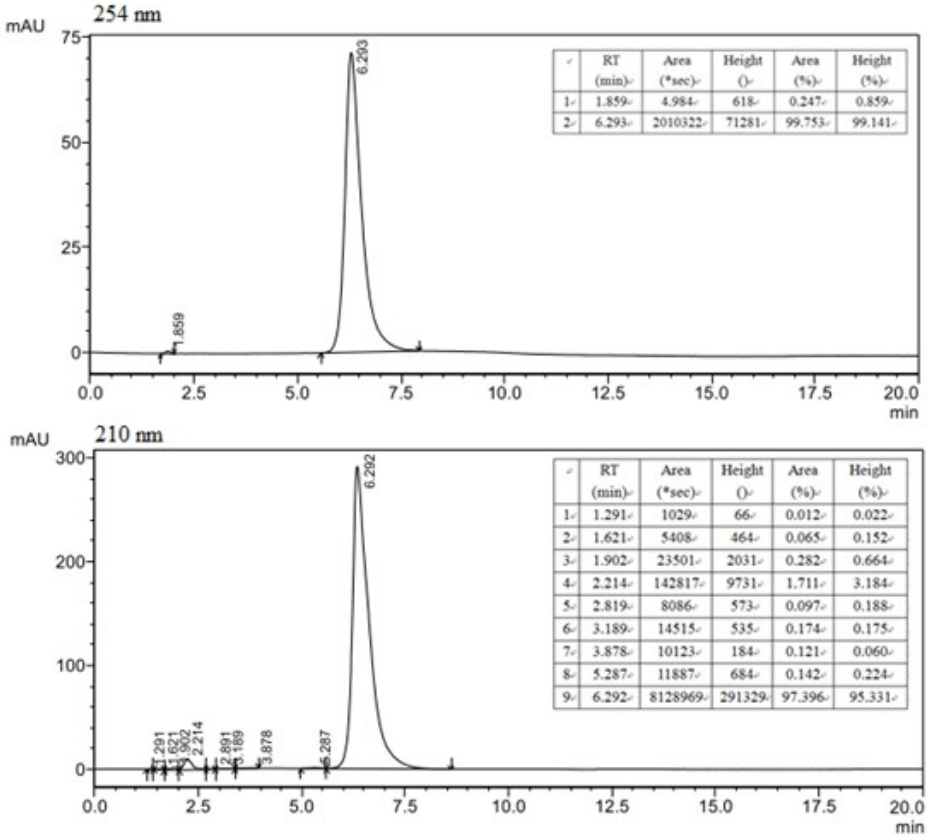

	RT (min)	Area (*sec)	Height ()	Area (%)	Height (%)
1	1.859	4.984	618	0.247	0.859
2	6.293	2010322	71281	99.753	99.141

	RT (min)	Area (*sec)	Height ()	Area (%)	Height (%)
1	1.291	1029	66	0.012	0.022
2	1.621	5408	464	0.065	0.152
3	1.902	23501	2031	0.282	0.664
4	2.214	142817	9731	1.711	3.184
5	2.819	8086	573	0.097	0.188
6	3.189	14515	535	0.174	0.175
7	3.878	10123	184	0.121	0.060
8	5.287	11887	684	0.142	0.224
9	6.292	8128969	291329	97.396	95.331

Figure S21. HPLC data of the target compound Ir-YC-1.

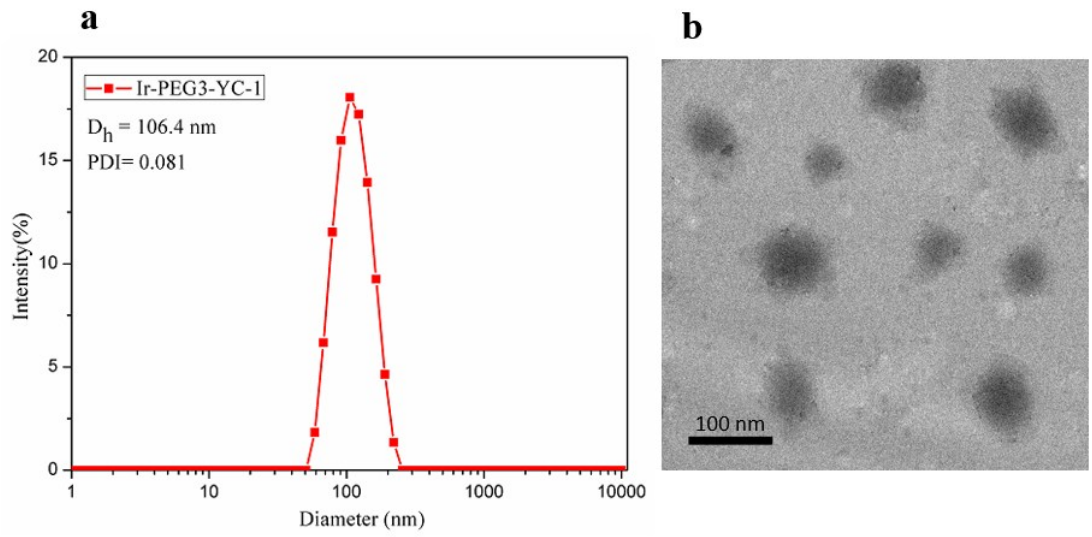

Figure S22. (a) Representative DLS profile and (b) TEM image of Ir-PEG_3-YC-1 nanoparticles.

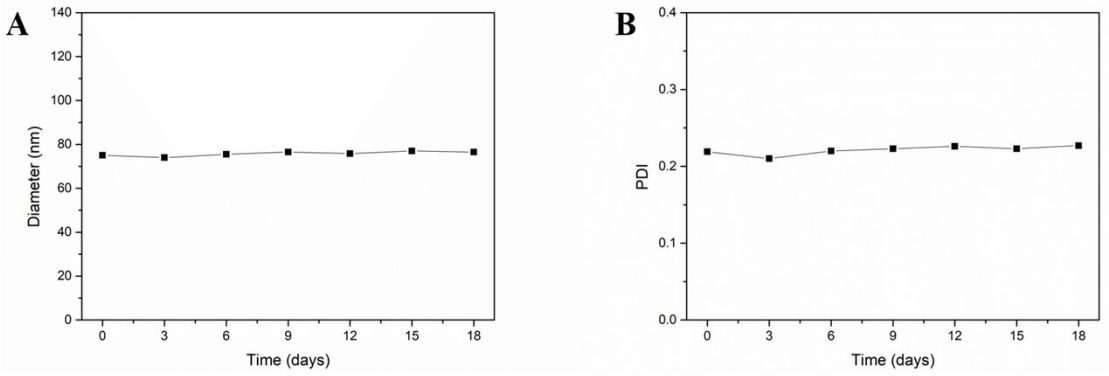

Figure S23. Influence of storage on diameter (A) and PDI (B) of Ir-YC-1 NPs. The solution of Ir-YC-1 NPs was stored at 4 °C in refrigerator for 18 days. At different time intervals (0, 3, 6, 9, 12, 15 and 18 d), the average size and PDI were determined. Samples were measured in triplicates. The values are the mean ± SD.

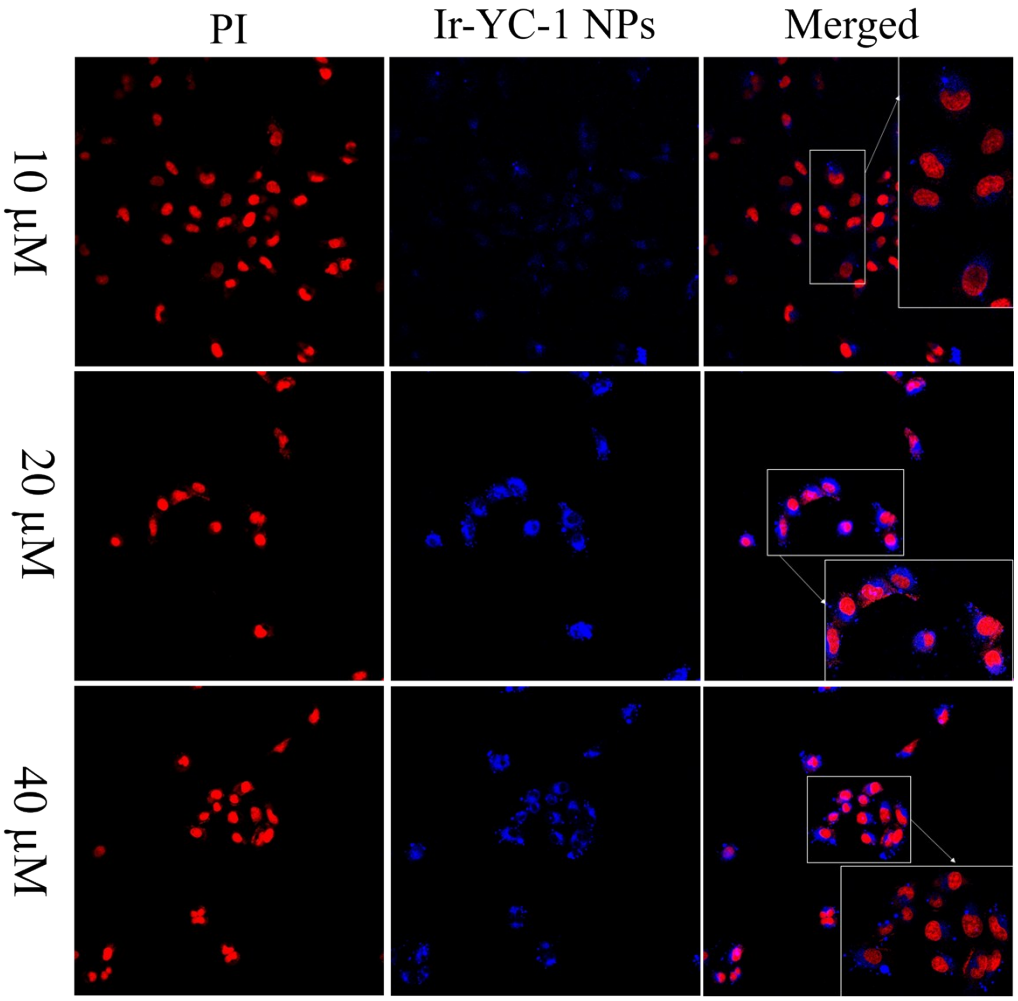

Figure S24. Cellular uptake of Ir-YC-1 NPs in A549 cells. Cell nuclei are stained with PI. CLSM photos of A549 cells incubated with Ir-YC-1 NPs for 2 h at 10, 20 and 40 μM under normoxia condition. Data represent three individual experiments.

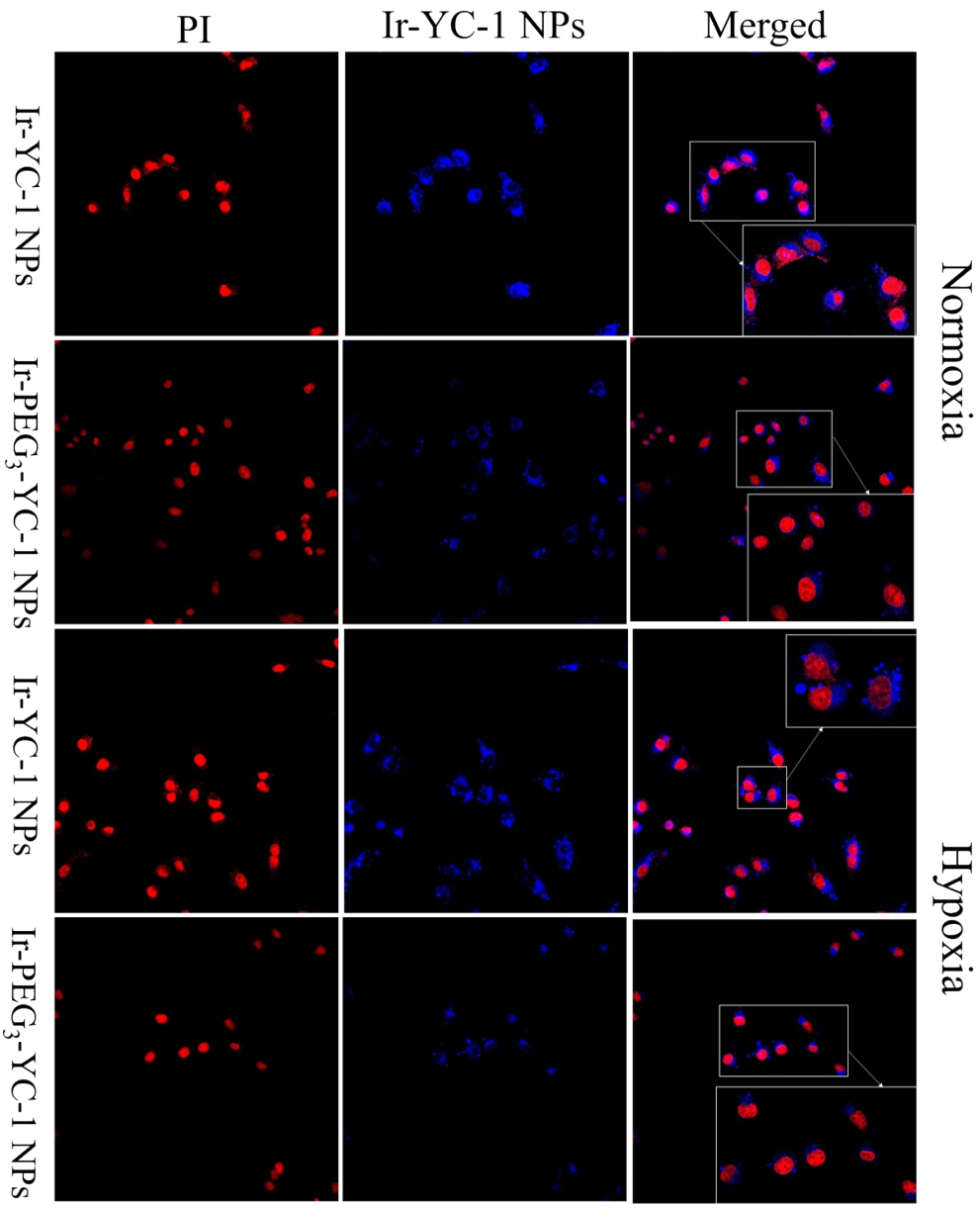

Figure S25. Cellular uptake of Ir-YC-1 and Ir-PEG_3-YC-1 NPs in A549 cells. Cell nuclei are stained with PI. CLSM photos of A549 cells incubated with Ir-YC-1 and Ir-PEG_3-YC-1 NPs for 2 h at 20 μM under normoxia or hypoxic condition. Data represent three individual experiments.

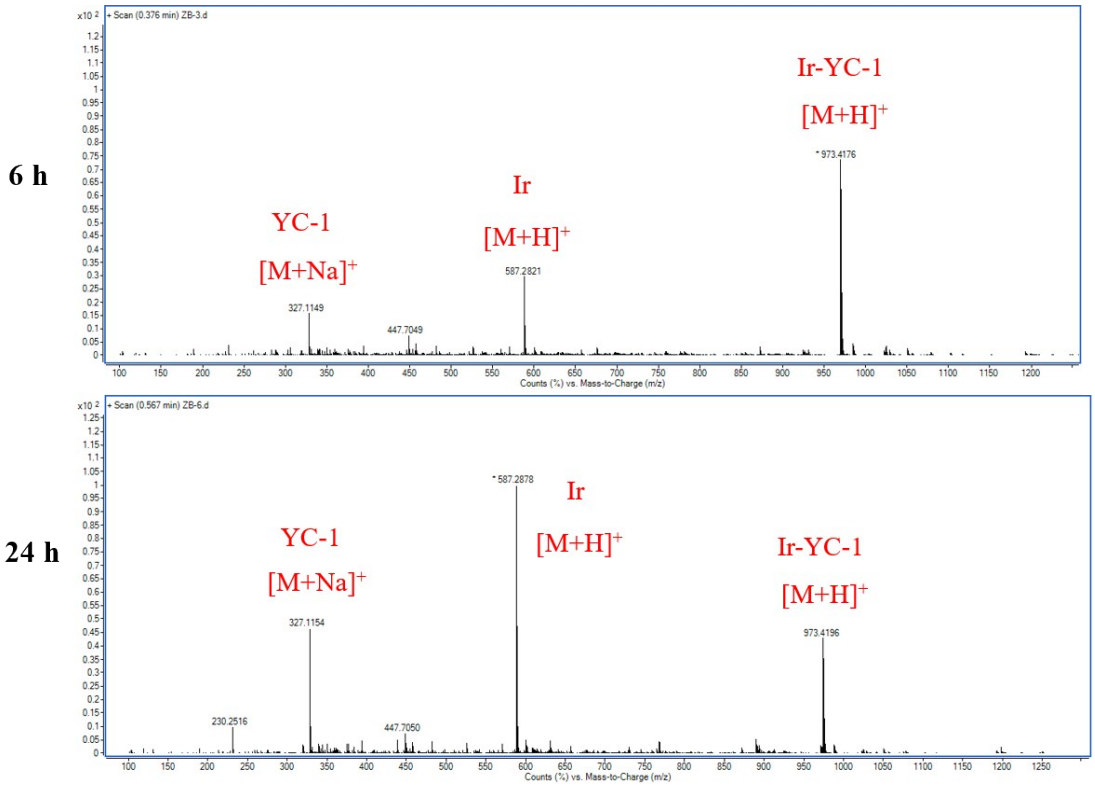

Figure S26. ESI-MS mass spectrum of Ir-YC-1 conjugate incubated with PBS (pH 5.0) for 6 h and 24 h at 37 °C.

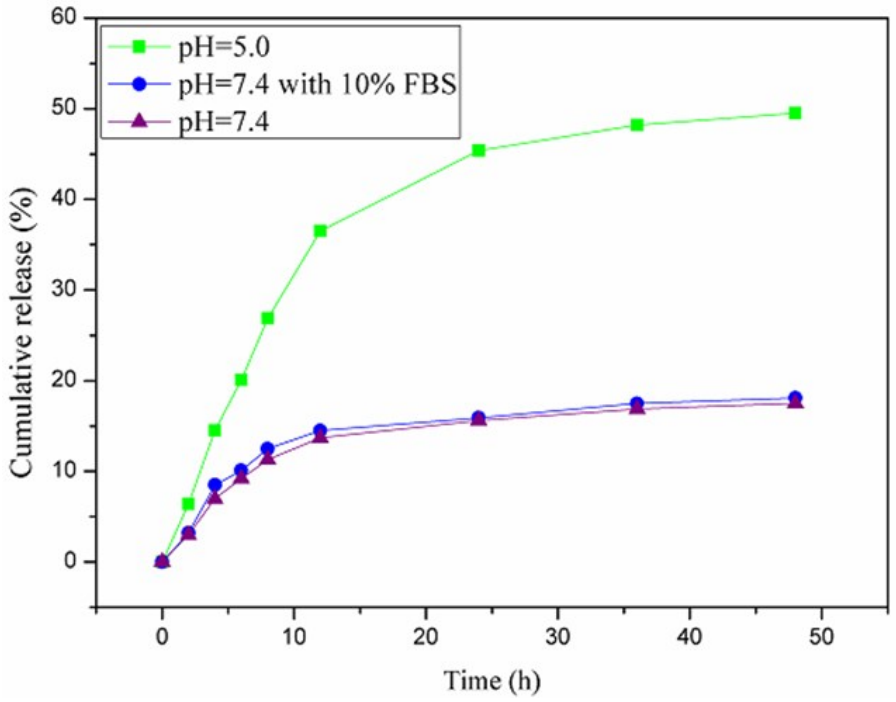

Figure S27. In vitro Ir release kinetics from Ir-YC-1 NPs under different pH values (5.0) and pH values (7.4) containing 10% FBS (or not) at 37 °C.

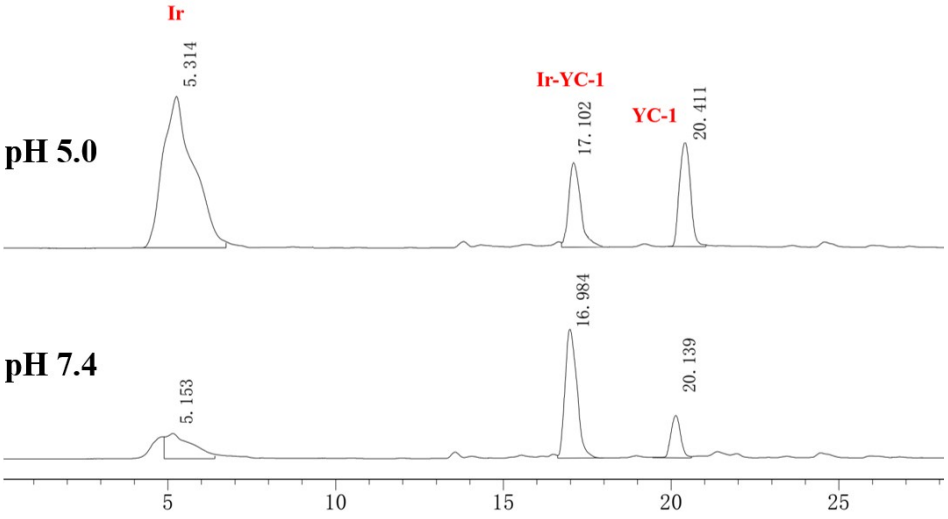

Figure S28. HPLC profiles of Ir-YC-1 NPs incubated with PBS (pH 7.4 or 5.0) at 37 °C for 48 h.

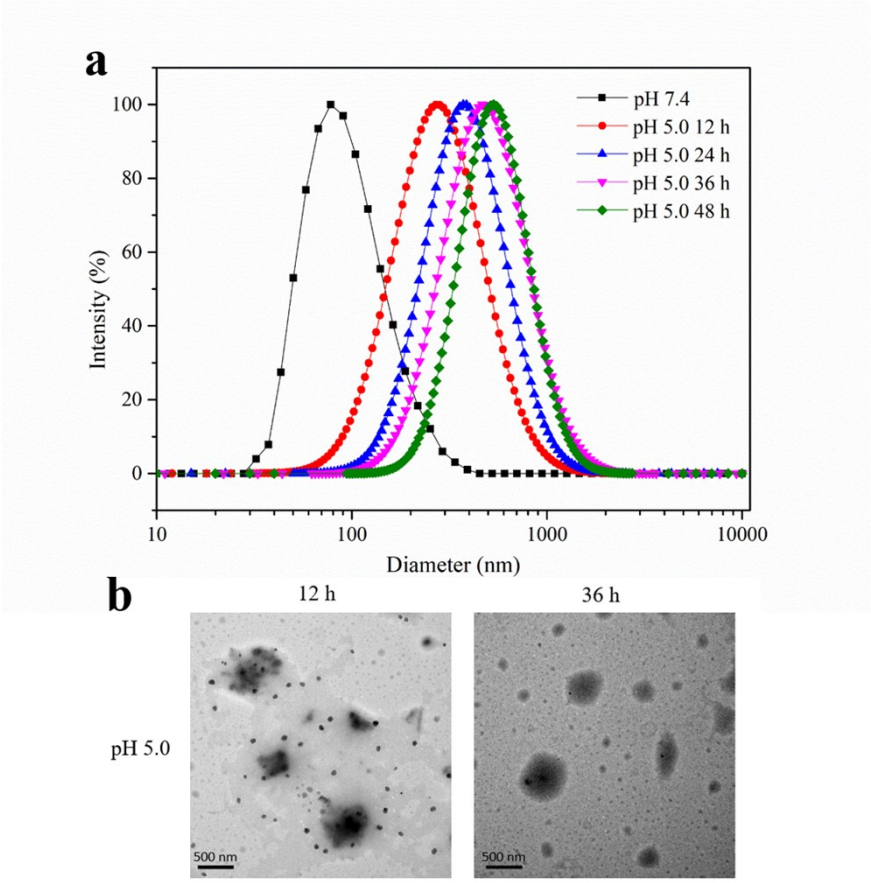

Figure S29. Diameter changes of Ir-YC-1 NPs in PBS (pH 5.0) at different time intervals determined by DLS (a) and TEM (b) measurements. Nanoparticles in PBS (pH 7.4) were used as a control.

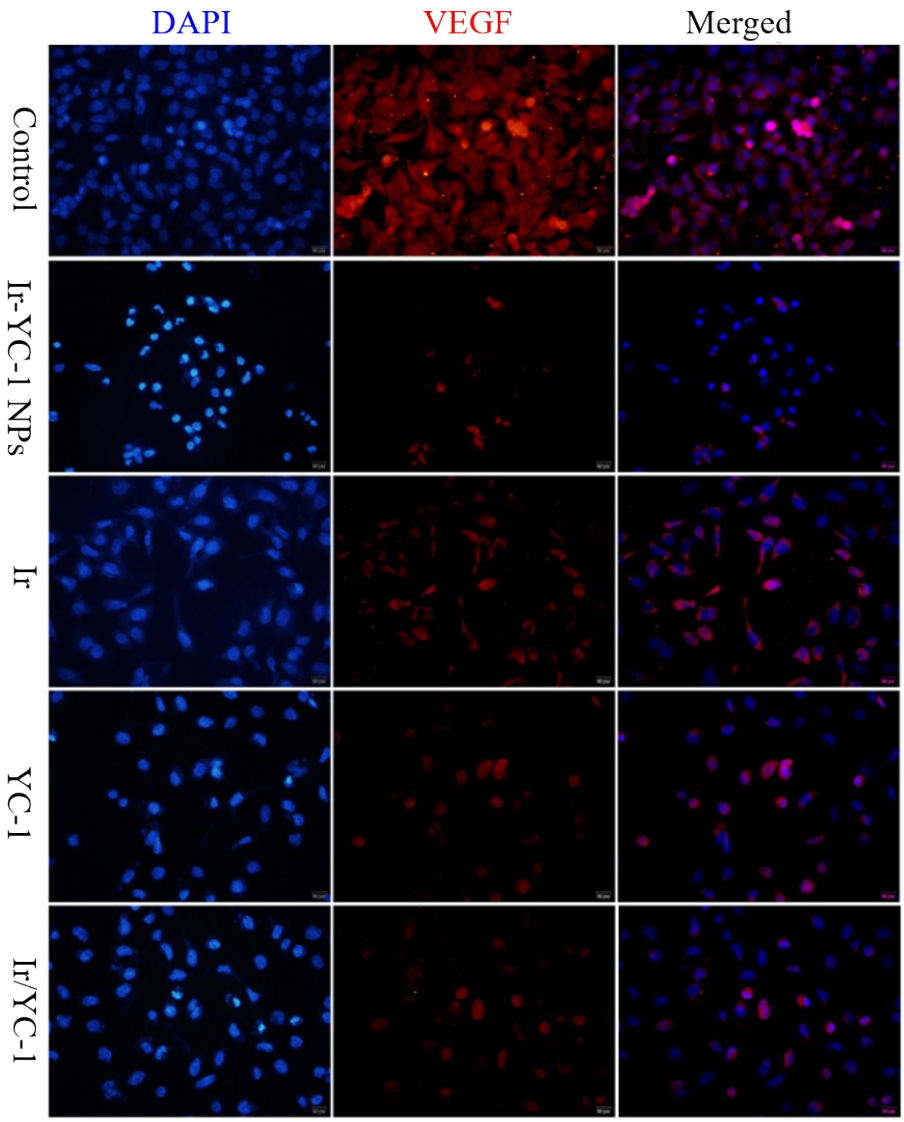

Figure S30. The accumulation of VEGF was examined in A549 cells treated with Ir, YC-1, Ir/YC-1 mixture, and Ir-YC-1 NPs, respectively, at the same concentration of 20 μM for 24 h under the hypoxic condition using immunofluorescence staining. Untreated cells served as negative control, Ir, YC-1 and Ir/YC-1 mixture acted as positive controls. Cells treated with the test compounds at the indicated concentration (20 μM) for 24 h were fixed in methanol and stained with VEGF and counterstained with 4, 6-diamidino-2-phenylindole (DAPI). The experiments were performed at least three times, and the results of the representative experiments were shown.

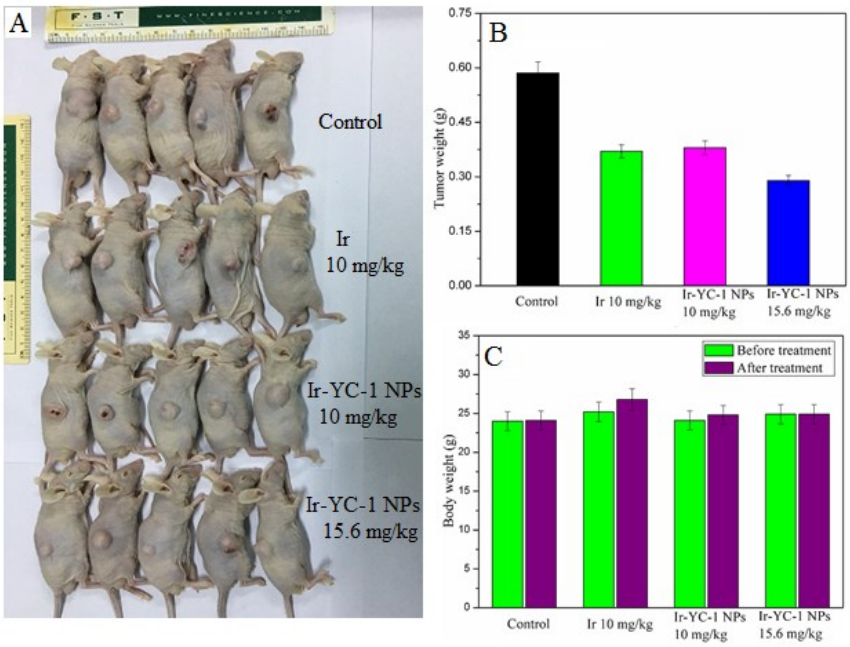

Figure S31. In vivo antitumor activity of Ir-YC-1 NPs in mice (BALB/c nude mice) bearing A549 xenograft model. (A) After administered with Ir-YC-1 NPs at the dose of 10 and 15.6 mg/kg for iv every 3 days for 28 days, Ir at the dose of 10 mg/kg for iv every 3 days for 28 days, the mice were sacrificed and weighed the tumors. (B) Mean weight of tumors separated from mice after different treatments. (C) The body weight of the mice recorded at the beginning and at the end of the treatments. Data are presented as the mean ± SEM of tumor volume and body weight at each time point for five animals per group: $p < 0.05$, vs control.

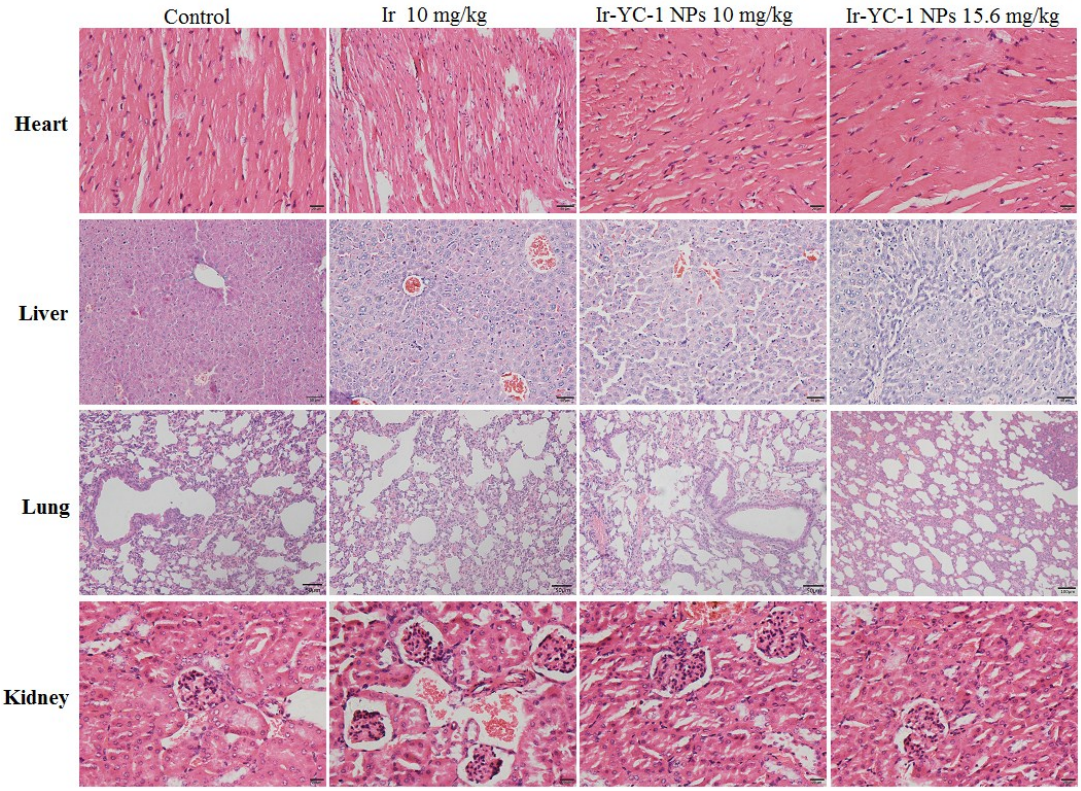

Figure S32. H&E staining indicated no obvious histopathological changes of major organs dissected from tumor-bearing mice after Ir and Ir-YC-1 NPs treatments. Scale bar = 20 μm.